Comparison of Synthetic Isoparaffinic Kerosene Turbine Fuels with the Composition-Explicit Distillation Curve Method

ARTICLE *in* ENERGY & FUELS · MARCH 2010

Impact Factor: 2.79 · DOI: 10.1021/ef100067q

3 AUTHORS, INCLUDING:

Thomas J Bruno
National Institute of Standards and Technol…
198 PUBLICATIONS **3,989** CITATIONS
SEE PROFILE

Tara M Lovestead
National Institute of Standards and Technol…
41 PUBLICATIONS **855** CITATIONS
SEE PROFILE

Energy Fuels **2010,** *24,* 3049–3059 · DOI:10.1021/ef100067q
Published on Web 04/01/2010

energy&fuels
article

Comparison of Synthetic Isoparaffinic Kerosene Turbine Fuels with the Composition-Explicit Distillation Curve Method

Thomas J. Bruno,* Evgenii Baibourine, and Tara M. Lovestead

Thermophysical Properties Division, National Institute of Standards and Technology, Boulder, Colorado

Received January 20, 2010. Revised Manuscript Received March 11, 2010

In recent years, civilian and military users of aviation kerosene have been interested in expanding the scope of fuel feed stocks to include nonpetroleum sources. There are many reasons for this, the most important of which are the potential minimization of supply disruptions, the minimization of dependence on foreign sources of petroleum, the vulnerability of large centralized refineries, and the rising costs of current fuel streams. It is unlikely that a completely new, drop-in replacement fuel will be successful in the foreseeable future. In the meantime, however, the goal is to extend or enhance present petroleum-derived stocks. For this to be done on a rational basis, careful attention must be paid to fuel design parameters, one of the most important of which is the fluid volatility as expressed by the distillation curve. We have recently introduced several important improvements in the measurement of distillation curves of complex fluids. The modifications to the classical measurement provide for (1) a composition explicit data channel for each distillate fraction (for both qualitative and quantitative analysis); (2) temperature measurements that are true thermodynamic state points that can be modeled with an equation of state; (3) temperature, volume, and pressure measurements of low uncertainty suitable for equation of state development; (4) consistency with a century of historical data; (5) an assessment of the energy content of each distillate fraction; (6) trace chemical analysis of each distillate fraction; and (7) a corrosivity assessment of each distillate fraction. The composition explicit channel is achieved with a new sampling approach that allows precise qualitative as well as quantitative analyses of each fraction, on the fly. We have applied the new method to the measurement of rocket propellant, gasolines, jet fuels, and hydrocarbon crude oils. In this paper, we present the application of the technique to compare the characteristics of several new synthetic isoparaffinic kerosenes that are being used or tested as turbine fuels. These fuels include synthetics made from natural gas, coal, and waste greases.

Introduction

In recent years, civilian and military users of aviation kerosene have been interested in expanding the scope of fuel feed stocks to include nonpetroleum sources. There are many reasons for this, the most important of which are guarding against potential supply disruptions, overcoming dependence on foreign sources of petroleum, overcoming the vulnerability of large centralized refineries (to both weather events and terrorist acts), and mitigation of the rising costs of current fuel streams.[1] Military users have additional incentives to explore alternatives. There is interest in developing fuel streams that can be manufactured in or near the theater of operations. This is currently not possible with petroleum-based fuels. Moreover, environmental regulation can limit operations (such as training exercises) with certain fuels that fail to meet emission targets. This has followed from provisions in the Energy Policy Act (EPAct) that promote increased alternative fuel percentages in the nontactical military fleet.[2] It is also clear that the demand for alternative fuels for gas turbine engines will increase in the near term.[3]

The two largest airframe manufacturers, Boeing and Airbus Industrie,[4] independently estimated the number of new civilian aircraft that will be needed in the next 20 years. To summarize the projected demand: approximately 17 500 single aisle, 6200 twin aisle, 1000 jumbo, and 3700 regional jets will be required in the world market.[5] The fuel requirement for the complete fleet is difficult to estimate, but a good projection is 177 million gallons per day worldwide. Approximately 40% of the world consumption of gas turbine fuel occurs in the United States, and of this, 90% is used by commercial carriers. This increased demand, as well as the noneconomic factors outlined above, drive the quest for alternative feedstocks.

Synthetic Isoparaffinic Kerosenes. Among the most promising alternative gas turbine fuels are the synthetic isoparaffinic kerosenes (S-IPK).[6,7] The most familiar of these fluids

*Author to whom correspondence should be addressed. E-mail: bruno@boulder.nist.gov.

(1) Muzzell, P. S. L.; Freerks, R.; McKay, B.; Terry, A.; Sattler, E. Properties of Fischer-Tropsch (FT) blends for use in military equipment. *SAE Paper No. 2006-01-1702*, 2006.

(2) Energy Policy Act of 2005, Public Law 109-58, Aug. 8, 2005.

(3) Daggett, D. L.; Hendricks, R. C.; Walther, R.; Corporan, E. *Alternate fuels for use in commercial aircraft*, NASA/TM-2008 214833, ISABE-2007−1196, 2008.

(4) Certain commercial equipment, materials, or supplies are identified in this paper to adequately specify the experimental procedure or description. Such identification does not imply recommendation or endorsement by the National Institute of Standards and Technology, nor does it imply that the equipment, materials, or supplies are the best available for the purpose.

(5) Fueling Green Aviation. *Flight Safety Australia* **2008**, May−June, 20−26.

(6) Moses, C. A.; Roets, P. N. J. *Comparative Evaluation of Semi-Synthetic Jet Fuels*, Final Report, Coordinating Research Council Project AV-2-04a, Dayton, OH, 2008.

(7) Rahmes, T. F.; Kinder, J D.; Henry, M.; Crenfeldt, G.; LeDuc, G. F.; Zombanakis, G. P.; Abe, Y.; Lambert, D. M.; Lewis, C.; Juenger, J. A.; Andac, M. G.; Reilly, K. R.; Holmgren, J.; McCall, M. J.; Bozzano, A. G. Sustainable bio-derived synthetic paraffinic kerosene (bio-SPK) jet fuel flight tests and engine program results. In *9th AIAA Aviation Technology, Integration and Operations Conference* (*ATIO*), American Institute for Aeronautics and Astronautics: Hilton Head, SC, 2009; Vol. 2009−7002, pp 1−19.

are prepared with the Fischer−Tropsch (FT) process, by which a synthesis gas (carbon monoxide and hydrogen) is converted into liquid hydrocarbons.[8,9] This gas can be obtained from the controlled combustion of natural gas, coal, or biomass. The conversion then occurs over iron or cobalt catalysts. A number of FT aviation fuels have been produced and studied. The most familiar is S-8, a natural gas derived FT fluid.[10−14] It is a synthetic substitute fluid for the military aviation fuel JP-8. Other processes to produce S-IPK fluids have emerged recently. In this paper, we compare several of these with FT fluids by use of the composition explicit distillation curve approach.

In earlier work, we presented extensive studies of FT fluid S-8, made from natural gas.[10−14] Here, we study another natural gas derived fluid, designated GTL. This fluid differs from S-8 in that it was made with the FT process over a low-temperature cobalt catalyst, producing C4 to C200 normal paraffins and olefins (called FT waxes). The resulting mixture was hydrocracked, isomerized, and fractionated to produce the isoparaffinic kerosene.

We also examined a biomass to liquid fuel (BIO-SPK). This fluid was converted to an isoparaffinic kerosene from a feed stock of animal fats, used cooking greases, and recovered brown greases. These feed stocks are lower in quality and cost than pure fats, at typically half the cost of fat from full-fat soybeans. The reaction is carried out by combined hydrodeoxygenation and hydrogenation (HDO) of fatty acids on a sulfided nickel molybdenum (NiMo) catalyst in a tubular reactor at a temperature of 400 °C (750 °F). This results in a stream of C14 to C18 normal paraffins that are then hydroisomerized and hydrocracked over a metallic catalyst (typically platinum) on a Lewis-acidic support (typically silica−alumina).

For comparison, we also present herein measurements on the commercial coal derived IPK fluid (CTL) made from coal with the FT process over a high-temperature iron catalyst.[15] This process results in a mixture of C1 to C4 olefins that are oligomerized, hydrogenated, and then fractionated to obtain the isoparaffinic kerosene. This mixture has been used in blends (to achieve the appropriate density and aromatic content specification) at OR Tambo International Airport (formerly Johannesburg International Airport) since 1999. More information about the composition of the fuels measured can be obtained from the corresponding author.

Advanced Distillation Curve Measurement. In earlier work, we described a method and apparatus for an advanced (or composition explicit) distillation curve (ADC) measurement that is especially applicable to the characterization of fuels. This method is a significant improvement over current approaches,[16] featuring (1) a composition explicit data channel for each distillate fraction (for both qualitative and quantitative analysis); (2) temperature measurements that are true thermodynamic state points that can be modeled with an equation of state; (3) temperature, volume, and pressure measurements of low uncertainty suitable for equation of state development; (4) consistency with a century of historical data; (5) an assessment of the energy content of each distillate fraction; (6) trace chemical analysis of each distillate fraction; and (7) a corrosivity assessment of each distillate fraction. The very significant advantage offered by the approach discussed in this paper is the ability to model the distillation curve resulting from our metrology with equation of state based models. Such thermodynamic model development is simply impossible with the classical approach to distillation curve measurement, or with any of the other techniques that are used to assess fuel volatility or vapor liquid equilibrium. We have applied this metrology to gasolines, diesel fuels, aviation fuels, and rocket propellants, and herein we apply it to several renewable gas turbine fuels.[10,12,14,17−41]

(8) Edwards, J. T. Advancements in gas turbine fuels from 1943 to 2005. *Trans. ASME* **2007**, *129* (1), 13–20.
(9) *MSDS, S-8 Synthetic Jet Fuel, material safety data sheet*; Syntroleum Corporation: Tulsa, OK, 2005.
(10) Bruno, T. J.; Smith, B. L. Improvements in the measurement of distillation curves - part 2: application to aerospace/aviation fuels RP-1 and S-8. *Ind. Eng. Chem. Res.* **2006**, *45*, 4381–4388.
(11) Bruno, T. J.; Laesecke, A.; Outcalt, S. L.; Seelig, H-D.; Smith, B. L. *Properties of a 50/50 Mixture of Jet-A + S-8, NIST-IR-6647*, 2007.
(12) Huber, M. L.; Smith, B. L.; Ott, L. S.; Bruno, T. J. Surrogate Mixture Model for the Thermophysical Properties of Synthetic Aviation Fuel S-8: Explicit Application of the Advanced Distillation Curve. *Energy Fuels* **2008**, *22*, 1104–1114.
(13) Outcalt, S. L.; Laesecke, A.; Freund, M. B. Density and speed of sound measurements of Jet A and S 8 aviation turbine fuels. *Energy Fuels* **2009**, *23* (3), 1626–1633.
(14) Smith, B. L.; Bruno, T. J. Application of a Composition-Explicit Distillation Curve Metrology to Mixtures of Jet-A + Synthetic Fischer−Tropsch S-8. *J. Propul. Power* **2008**, *24* (3), 619–623.
(15) Moses, C. A., Roets, P. N. J. Properties characteristics and combustion performance of Sasol fully synthetic jet fuel. *J. Eng. Gas Turb. Power* **2009**, *131* (July), 041502-1−041502-17.
(16) *ASTM Standard D 86−04b, Standard Test Method for Distillation of Petroleum Products at Atmospheric Pressure*; ASTM International: West Conshohocken, PA, 2004.
(17) Bruno, T. J. Improvements in the measurement of distillation curves - part 1: a composition-explicit approach. *Ind. Eng. Chem. Res.* **2006**, *45*, 4371–4380.
(18) Bruno, T. J. Method and apparatus for precision in-line sampling of distillate. *Sep. Sci. Technol.* **2006**, *41* (2), 309–314.
(19) Huber, M. L.; Lemmon, E. W.; Diky, V.; Smith, B. L.; Bruno, T. J. Chemically authentic surrogate mixture model for the thermophysical properties of a coal-derived-liquid fuel. *Energy Fuels* **2008**, *22*, 3249–3257.
(20) Huber, M. L.; Lemmon, E.; Kazakov, A.; Ott, L. S.; Bruno, T. J. Model for the thermodynamic properties of a biodiesel fuel. *Energy Fuels* **2009**, *23*, 3790–3797.
(21) Huber, M. L.; Lemmon, E.; Ott, L. S.; Bruno, T. J. Preliminary surrogate mixture models for rocket propellants RP-1 and RP-2. *Energy Fuels* **2009**, *23*, 3083–3088.
(22) Huber, M. L.; Lemmon, E.; Bruno, T. J. Effect of RP-1 compositional variability on thermophysical properties. *Energy Fuels* **2009**, *23*, 5550–5555.
(23) Lovestead, T. M.; Bruno, T. J. Application of the advanced distillation curve method to aviation fuel avgas 100LL. *Energy Fuels* **2009**, *23*, 2176–2183.
(24) Lovestead, T. M.; Bruno, T. J. Comparison of the hypersonic vehicle fuel JP-7 to the rocket propellants RP-1 and RP-2 with the advanced distillation curve method. *Energy Fuels* **2009**, *23* (7), 3637–3644.
(25) Ott, L. S.; Bruno, T. J. Corrosivity of fluids as a function of distillate cut: application of an advanced distillation curve method. *Energy Fuels* **2007**, *21*, 2778–2784.
(26) Ott, L. S.; Smith, B. L.; Bruno, T. J. Advanced distillation curve measurements for corrosive fluids: application to two crude oils. *Fuel* **2008**, *87*, 3055–3064.
(27) Ott, L. S.; Smith, B. L.; Bruno, T. J. Advanced distillation curve measurement: application to a bio-derived crude oil prepared from swine manure. *Fuel* **2008**, *87*, 3379–3387.
(28) Ott, L. S.; Smith, B. L.; Bruno, T. J. Composition-explicit distillation curves of mixtures of diesel fuel with biomass-derived glycol ester oxygenates: a fuel design tool for decreased particulate emissions. *Energy Fuels* **2008**, *22*, 2518–2526.
(29) Ott, L. S.; Hadler, A.; Bruno, T. J. Variability of the rocket propellants RP-1, RP-2, and TS-5: application of a composition- and enthalpy-explicit distillation curve method. *Ind. Eng. Chem. Res.* **2008**, *47* (23), 9225–9233.
(30) Ott, L. S.; Bruno, T. J. Variability of biodiesel fuel and comparison to petroleum-derived diesel fuel: application of a composition and enthalpy explicit distillation curve method. *Energy Fuels* **2008**, *22*, 2861–2868.
(31) Smith, B. L.; Bruno, T. J. Advanced distillation curve measurement with a model predictive temperature controller. *Int. J. Thermophys.* **2006**, *27*, 1419–1434.

Moreover, the method has also been applied to the volatility simulation of heavy oils.[42]

Experimental Section

The aviation fuels used in this work (GTL, CTL, and BIO-SPK) were obtained from the Propulsion Directorate of the Air Force Research Laboratory at Wright Patterson Air Force Base in Ohio. These fluids were stored at 7 °C to preserve any volatile components. No phase separation was observed as a result of this storage procedure. Each fuel was examined by gas chromatography (30 m capillary column of 5% phenyl−95% dimethyl polysiloxane having a thickness of 1 μm, flame ionization detection and mass spectrometric detection). The temperature programs differed slightly in order to optimize the chromatography for each of the fuels (GTL: 70 °C for 2 min, 9 °C per min to 100 °C, 4 °C per min to 210; CTL: 40 °C for 2 min, 3 °C per min to 145 °C; BIO-SPK: 70 °C for 2 min, 9 °C per min to 100 °C, 4 °C per min to 210 °C).[43,44] Following each temperature program, the column was maintained at 250 °C for several minutes to ensure a complete column cleanup. In Table 1a−c, we present a listing of the compounds found to be in excess of 1.5% of the total uncorrected area counts listed in order of retention time. Identifications were made on the basis of the mass spectra, with the aid of the NIST/EPA/NIH Mass Spectral Database,[45] and also on the basis of retention indices. These analytical results (compositions and relative quantities of components) are consistent with our knowledge of the nature of the feedstock and the processing used to obtain each fluid.

Table 1. Listing of the Major Components in (a) GTL Fuel, (b) CTL Fuel, and (c) BIO-SPK Fuel[a]

RT (min)	compound	CAS No.	RMM	area %
	(a) GTL Fuel			
1.482	*n*-hexane	110−54−3	86.18	3.3
2.444	*n*-octane	111−65−9	114.23	1.5
3.140	2,3,4-trimethyl hexane	921−47−1	128.16	3.5
3.233	3-methyl octane	2216−33−3	128.16	2.3
3.642	*n*-nonane	111−84−2	128.16	10.4
4.125	3,6-dimethyl octane	15869−94−0	142.28	6.4
4.626	2-methyl nonane	871−83−0	142.28	12.3
4.750	3-methyl nonane	5911−09−6	142.28	4.7
5.284	*n*-decane	124−18−5	142.28	14.5
5.482	4,5-dimethyl nonane	17302−23−7	156.31	4.2
5.735	2,6-dimethyl octane	17302−28−2	156.31	1.7
5.856	3,7-dimethyl nonane	17302−32−8	156.31	2.8
6.189	5-ethyl-2-methyl octane	62016−18−6	156.31	1.9
6.446	2-methyl decane	6975−98−0	156.31	8.2
6.578	3-methyl decane	13151−34−3	156.31	3.2
7.195	*n*-undecane	1120−21−4	156.31	5.1
7.553	2,5-dimethyl decane	17312−50−4	170.33	2.9
8.443	5-methyl undecane	1632−70−8	170.33	2.2
	(b) CTL Fuel			
7.682	2,3-dimethyl octane	7146−60−3	142.28	2.9
8.010	2,3,4-trimethyl heptane	52896−95−4	142.28	1.8
9.408	2,5-dimethyl octane	15869−89−3	142.28	2.0
9.944	2,6-dimethyl octane	2051−30−1	142.28	1.8
10.148	x-methyl nonane	N/A	142.28	2.1
10.661	5-ethyl-2-methyl heptane	13475−78−0	142.28	1.6
10.843	3,3,5-trimethyl heptane	7154−80−5	142.28	1.6
11.187	*n*-decane	124−18−5	142.28	2.1
11.754	2,5,6-trimethyl octane	62016−14−2	156.31	5.3
12.235	2,2,6,6-tetramethyl heptane	40177−45−1	156.31	1.6
12.532	2,4,6-trimethyl octane	62016−37−9	156.31	2.2
13.532	3,7-dimethyl nonane	17302−32−8	156.31	2.8
14.584	x-methyl decane	N/A	156.31	2.2
14.838	2,3,7-trimethyl octane	62016−34−6	156.31	1.8
15.172	x-methyl decane	N/A	156.31	3.2
15.787	*n*-undecane	1120−21−4	156.31	1.6
17.035	3,8-dimethyl decane	17312−55−9	170.33	1.6
18.980	x-methyl undecane	N/A	170.33	1.9
27.052	4,6-dimethyl undecane	17312−82−2	184.36	1.7
	(c) BIO-SPK Fuel			
3.204	4-methyl octane	2216−34−4	128.16	2.0
4.165	2,6-dimethyl octane	2051−30−1	142.28	1.6
4.668	4-methyl nonane	17301−94−9	142.28	2.4
4.793	3-methyl nonane	5911−04−6	142.28	1.5
5.620	2,5 dimethyl nonane	17302−27−1	156.31	1.9
6.495	2-methyl decane	6975−98−0	156.31	2.7
6.624	3-methyl decane	13151−34−3	156.31	1.7
7.257	*n*-undecane	1120−21−4	156.31	2.2
7.593	3,6-dimethyl decane	17312−53−7	170.33	1.9
8.502	5-ethyl decane	17302−36−2	170.33	3.0
8.878	3-methyl undecane	1002−43−3	170.33	2.6
9.655	*n*-dodecane	112−40−3	170.33	2.3
9.982	2,3,5 trimethyl decane	62238−11−3	184.36	2.7
11.031	5-methyl dodecane	17453−93−9	184.36	2.3
12.368	*n*-tridecane	629−50−5	184.36	3.3
12.810	6-methyl tridecane	13287−21−3	198.39	1.9
13.856	2,5 dimethyl dodecane	56292−65−0	198.39	2.5
14.362	3-methyl tridecane	6418−41−8	198.39	1.8
15.241	*n*-tetradecane	629−54−4	198.39	2.2
16.643	*n*-pentadecane	629−62−9	212.41	2.2

[a] This analysis was done by GC-MS (30 m capillary column of 5% phenyl−95% dimethyl polysiloxane having a thickness of 1 μm, column temperature programmed for 70 °C for 2 minutes, 9 °C per min to 100 °C, 4 °C per min to 210 °C). The area % data presented here are the raw, uncorrected areas, and RMM is the relative molecular mass. Note that it is not always possible to determine the position of methyl substitution, and in these instances the position is indicated with an "x".

We will note later in this paper that these analyses are also consistent with the results from the composition explicit data

(32) Smith, B. L.; Bruno, T. J. Improvements in the measurement of distillation curves: part 3 - application to gasoline and gasoline + methanol mixtures. *Ind. Eng. Chem. Res.* **2007**, *46*, 297–309.
(33) Smith, B. L.; Bruno, T. J. Improvements in the measurement of distillation curves: part 4- application to the aviation turbine fuel Jet-A. *Ind. Eng. Chem. Res.* **2007**, *46*, 310–320.
(34) Smith, B. L.; Bruno, T. J. Composition-explicit distillation curves of aviation fuel JP-8 and a coal based jet fuel. *Energy Fuels* **2007**, *21*, 2853–2862.
(35) Smith, B. L.; Ott, L. S.; Bruno, T. J. Composition-explicit distillation curves of diesel fuel with glycol ether and glycol ester oxygenates: a design tool for decreased particulate emissions. *Environ. Sci. Technol.* **2008**, *42* (20), 7682–7689.
(36) Smith, B. L.; Ott, L. S.; Bruno, T. J. Composition-explicit distillation curves of commercial biodiesel fuels: comparison of petroleum derived fuel with B20 and B100. *Ind. Eng. Chem. Res.* **2008**, *47* (16), 5832–5840.
(37) Bruno, T. J.; Wolk, A.; Naydich, A. Stabilization of biodiesel fuel at elevated Temperature with Hydrogen Donors: evaluation with the advanced distillation curve method. *Energy Fuels* **2009**, *23*, 1015–1023.
(38) Bruno, T. J.; Wolk, A.; Naydich, A. Composition-explicit distillation curves for mixtures of gasoline with four-carbon alcohols (butanols). *Energy Fuels* **2009**, *23*, 2295–2306.
(39) Bruno, T. J.; Wolk, A.; Naydich, A. Analysis of fuel ethanol plant liquor with the composition explicit distillation curve approach. *Energy Fuels* **2009**, *23* (6), 3277–3284.
(40) Bruno, T. J.; Wolk, A.; Naydich, A.; Huber, M. L. Composition explicit distillation curves for mixtures of diesel fuel with dimethyl carbonate and diethyl carbonate. *Energy Fuels* **2009**, *23* (8), 3989–3997.
(41) Hadler, A. B.; Ott, L. S.; Bruno, T. J. Study of azeotropic mixtures with the advanced distillation curve approach. *Fluid Phase Equilib.* **2009**, *281*, 49–59.
(42) Satyro, M. A.; Yarranton, H Oil characterization from simulation of experimental distillation data. *Energy Fuels* **2009**, *23*, 3960–3970.
(43) Bruno, T. J.; Svoronos, P. D. N. *CRC Handbook of Basic Tables for Chemical Analysis*, 2nd. ed.; Taylor and Francis CRC Press: Boca Raton, FL, 2004.
(44) Bruno, T. J.; Svoronos, P. D. N. *CRC Handbook of Fundamental Spectroscopic Correlation Charts*; Taylor and Francis CRC Press: Boca Raton, FL, 2005.
(45) *NIST/EPA/NIH Mass Spectral Database, S. R. D.*; SRD Program, National Institute of Standards and Technology: Gaithersburg, MD, 2005.

channel of the ADC. No dye or taggant was found in any of the fluids.

The *n*-hexane used as a solvent in this work was obtained from a commercial supplier and was analyzed by gas chromatography (30 m capillary column of 5% phenyl−95% dimethyl polysiloxane having a thickness of 1 μm, temperature program from 50 to 170 °C, 5 °C per minute) with flame ionization detection and mass spectrometric detection. These analyses revealed the purity to be approximately 99.9%, and the fluid was used without further purification.

The method and apparatus for the distillation curve measurement has been reviewed in a number of sources (see refs 10−40), so an additional general description will not be provided here. The required volume of fluid for the distillation curve measurement (in each case, 200 mL) was placed into the boiling flask with a 200 mL volumetric pipet and an automatic pipetter. The thermocouples were then inserted into the proper locations to monitor T_k, the temperature in the fluid, and T_h, the temperature at the bottom of the takeoff position in the distillation head. Enclosure heating was then commenced with a four-step program based upon a previously measured distillation curve. This program was designed to impose a heating profile on the enclosure that led the fluid temperature by approximately 20 °C. Volume measurements were made in the level-stabilized receiver, and sample aliquots were collected at the receiver adapter hammock. In the course of this work, we performed between four and six complete distillation curve measurements for each of the fluid samples.

Since the measurements of the distillation curves were performed at ambient atmospheric pressure (measured with an electronic barometer), temperature readings were corrected for what should be obtained at standard atmospheric pressure (1 atm = 101.325 kPa). This adjustment was done with the modified Sydney Young equation, in which the constant term was assigned a value of 0.000109.[46−49] This value corresponds to a carbon chain of 12. In the chemical analysis of the aviation fuel samples (see above), as well as in previous work on aviation turbine fuel, it was found that *n*-dodecane can indeed represent the fluid as a very rough surrogate.[50,51] The magnitude of the correction is of course dependent upon the extent of departure from standard atmospheric pressure. The location of the laboratory in which the measurements reported herein were performed is approximately 1650 m above sea level, resulting in a typical temperature adjustment of 7 °C. The actual measured temperatures are easily recovered from the Sydney Young equation at each measured atmospheric pressure.

Results and Discussion

Initial Boiling Temperatures. During the initial heating of each sample during the distillation, the behavior of the fluid was carefully observed. Direct observation through the bore scope ports allowed the measurement of the onset of boiling behavior for each fluid. Typically, during the earlier stages of a measurement, the first bubbles will appear intermittently and are rather small. These bubbles cease if the stirrer is stopped momentarily. The temperature at which this bubbling is observed is called the onset temperature, and it is typically associated with the release of dissolved atmospheric gases and very light hydrocarbon gases. Sustained bubbling, which occurs subsequent to onset, is characterized by larger, more vigorous bubbles and is still observed when the stirring is briefly stopped. Finally, vapor is observed to rise into the distillation head, causing an immediate response on the T_h thermocouple. This temperature has been shown to be the initial boiling temperature (IBT) of the fluid. Furthermore, this temperature is of low uncertainty and thermodynamically consistent, and it can therefore be modeled theoretically with an equation of state. Experience with previous mixtures, including *n*-alkane standard mixtures that were prepared gravimetrically, indicates that the uncertainty in the onset of the bubbling temperature is approximately 2 °C. The uncertainty in the vapor rise temperature is 0.3 °C. The uncertainty in the pressure measurement (assessed by logging a pressure measurement every 15 s for the duration of a typical distillation) is 0.001 kPa.

Table 2. Comparison of the Initial Boiling Temperatures of the Three Fuels: GTL, CTL, and BIO-SPK[a]

observed temperature	GTL, °C (82.31 kPa)	CTL, °C (83.90 kPa)	BIO-SPK, °C (83.13 kPa)
onset	155	124	141
sustained	166	171	185
vapor rise	**166.2**	**172.3**	**188.4**

[a] These temperatures have been corrected to 1 atm with the Sydney Young equation. The pressures at which the measurements were made are provided for each fuel to permit recovery of the actual measured temperature. The uncertainty (with a coverage factor $k = 2$) in the onset and sustained bubbling temperatures is ~2 °C. The uncertainty in the vapor rise temperature is actually much lower, at ~0.3 °C.

The initial temperature observations (onset, sustained, and vapor rise) for a representative measurement are summarized in Table 2. For example, in the case of the GTL fluid, the temperature for the appearance of the first vapor bubble was 155.4 °C, measured in the fluid by the thermocouple recording T_k. Sustained bubbling was observed when the temperature of the fluid reached 165.8 °C. Vapor rising into the distillation head was then observed at 166.2 °C. These temperatures have been corrected to atmospheric pressure with the modified Sydney Young equation, as described above. The most important of the initial boiling behavior temperatures are the vapor rise temperatures, which have been illustrated as histograms for all the fluids in Figure 1. The vapor rise temperatures of GTL and CTL are comparable, but the modest difference shows that CTL has a relatively greater concentration of lower volatility compounds. In contrast, the biomass fuel (BIO-SPK) exhibits a much higher vapor rise temperature. This suggests that it has a composition that is made up of an even higher concentration of lower volatility, higher relative molecular mass compounds.

Distillation Curves. During the measurement of the distillation curves, both the kettle and head temperatures were recorded. The ambient pressure was also recorded and used to correct the temperatures to atmospheric pressure by use of the modified Sydney Young equation. Fluid and head temperatures, as well as the measured atmospheric pressure,

(46) Ott, L. S.; Smith, B. L.; Bruno, T. J. Experimental test of the Sydney Young equation for the presentation of distillation curves. *J. Chem. Thermodyn.* **2008**, *40*, 1352–1357.
(47) Young, S. Correction of boiling points of liquids from observed to normal pressures. *Proc. Chem. Soc.* **1902**, *81*, 777.
(48) Young, S. *Fractional distillation*; Macmillan and Co., Ltd.: London, 1903.
(49) Young, S. *Distillation principles and processes*; Macmillan and Co., Ltd.: London, 1922.
(50) Huber, M. L.; Laesecke, A.; Perkins, R. A. Transport properties of dodecane. *Energy Fuels* **2004**, *18*, 968–975.
(51) Lemmon, E. W.; Huber, M. L. Thermodynamic properties of n-dodecane. *Energy Fuels* **2004**, *18*, 960–967.

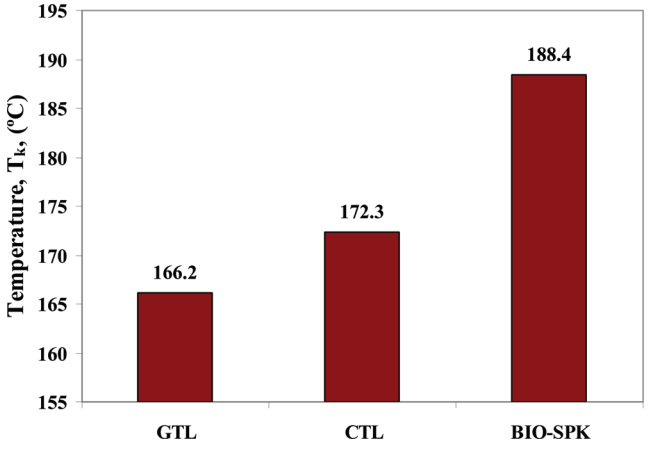

Figure 1. Comparison of the vapor rise temperature of the three fuels, studied: GTL, CTL, and BIO-SPK. The uncertainty is discussed in the text and is ~0.3 °C.

are presented as a function of distillate cut for a representative measurement for each fluid in Table 3. One can observe that the different fuels have very different temperature ranges: GTL distills over a range of 20 °C, while BIO-SPK distills over a range of 80 °C during the course of distillation. The range of temperatures during a distillation is related to the number of compounds that differ in volatility. The greater temperature range of BIO-SPK suggests that this fluid contains compounds of a wider range of volatilities than either GTL or CTL. Note that this observation is consistent with the components found in the neat fuel samples presented in Table 1.

The distillation measurements of each fuel were performed four times. The temperatures for each distillate fraction were averaged across the four measurements, and the standard deviation was also determined. It was found that the curves were highly reproducible. In our previous work with the ADC, we reported a maximum uncertainty in temperatures of 0.3 °C. In this work, the average standard deviation for each point in T_k was somewhat better at 0.13 °C. The uncertainty in the volume measurement that is used to obtain the distillate volume fraction is 0.05 mL in each case. The relatively low uncertainties in the measured quantities facilitate modeling the results, for example with an equation of state.

The data in Table 3 are presented graphically in Figure 2. The shapes of the curves are subtle sigmoids, consistent with the known fact that they are relatively complex fluid mixtures. The volatility differences among the fluids are clearly shown. The curves of two isoparaffinic kerosenes, GTL and CTL, are largely flat throughout the distillation, exhibiting little temperature change. The distillation curve of BIO-SPK is very different. While this curve begins with a gentle slope, a far more pronounced curvature develops later in the distillation. The significant difference in the range of temperatures is now visually apparent. The shape of the distillation curve of BIO-SPK as well as the temperature range suggest that BIO-SPK has a greater number of relatively low volatility compounds.

We point out that our measurements of T_h are similar to what one would obtain with the classical apparatus. The parallels can be seen by comparison to curves measured in this way.[52]

Table 3. Representative Distillation Curve Data for the Three Fuels[a]

distillate volume fraction, %	GTL (82.31 kPa)		CTL (83.59 kPa)		BIO-SPK (83.13 kPa)	
	T_k, °C	T_h, °C	T_k, °C	T_h, °C	T_k, °C	T_h, °C
5	166.9	163.3	173.9	167.7	192.6	172.5
10	167.5	164.2	175.2	169.1	196.8	180.5
15	168.4	165.1	176.3	170.3	200.6	186.5
20	169.1	166.0	177.6	172.1	204.4	189.9
25	169.8	166.5	179.1	173.7	208.7	194.9
30	170.5	166.8	180.6	175.3	213.1	201.2
35	171.4	167.5	182.0	177.0	217.5	206.1
40	172.3	168.3	183.6	178.7	221.8	210.3
45	173.2	169.6	185.3	180.7	226.3	215.4
50	174.4	170.0	187.2	182.7	231.1	219.2
55	175.9	172.8	189.1	184.5	235.5	224.7
60	176.9	174.0	190.9	186.9	240.3	231.4
65	178.1	175.8	192.9	189.2	244.8	235.7
70	179.5	177.2	195.9	192.0	249.7	242.5
75	181.1	178.7	198.9	195.0	254.6	246.8
80	182.3	181.1	202.1	198.3	259.4	251.6
85	184.6	183.6	206.5	202.6	264.7	257.8
90	186.3	186.3	212.4	206.9	270.1	264.1

[a] The uncertainties are discussed in the text. These temperatures have been adjusted to 1 atm with the Sydney Young equation; the experimental atmospheric pressures are provided to allow recovery of the actual measured temperatures.

Composition Explicit Data Channel. As described in the Experimental Section, sample aliquots of 7 μL were taken during the course of the distillation at selected volume fractions. These were then dissolved in a known mass of solvent (*n*-hexane). This solvent was chosen because it does not interfere with the subsequent analysis. The chromatographic peak of *n*-hexane elutes before the components of the fuels, so the solvent does not hamper the examination of the fuel components. The samples were analyzed by the GC-MS. Chromatograms, presented as total ion chromatograms (TICs), were obtained for these fractions by the same method (30 m capillary column of 5% phenyl−95% dimethyl polysiloxane having a thickness of 1 μm, temperature program from 70 to 100 °C, 9 °C per minute, 100 to 210 °C, 4 °C per minute) on the same column. In Figure 3, we present TICs for each fluid at the 0.0025% (first drop), 10%, 50%, 70%, and 90% volume fractions. The time axis is from 2 to 25 min for each chromatogram, and the abundance axis is presented in arbitrary units of area counts (voltage slices). These particular fractions were chosen to best illustrate the composition differences between the fluids. A few of the major peaks are labeled as to composition. The compositional differences are seen in the curves where the curves diverge the most, and where the curvature or slope is most pronounced. This chromatographic analysis, together with the fragmentation data from the mass spectrometer, provides a way to identify and track the components of the fuels through the progression of the distillation curves.

For GTL, the dominant component is *n*-nonane for the first drop, 10%, and 50% distillate fractions. After those fractions, *n*-decane becomes the dominant peak. Besides these two components, the other (less abundant) peaks are substituted C_9, C_{10}, and C_{11} compounds. The composition of GTL remains relatively constant throughout the distillation, and this is reflected in the modest range of temperatures in the distillation curve. The volatilities of *n*-nonane and *n*-decane are comparable, and their boiling points are relatively

(52) Moses, C. A. *Comparative Evaluation of Semi-synthetic Jet Fuels, Addendum: Further Analysis of Hydrocarbons and Trace Materials to Support D7566*, Final Report, Coordinating Research Council Project AV-2-04a, 2009.

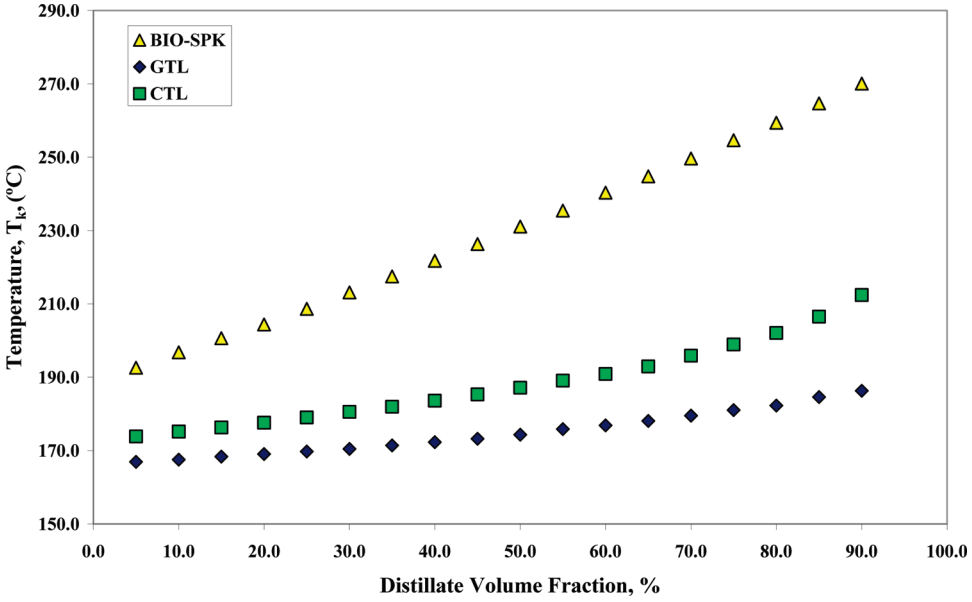

Figure 2. Representative distillation curves of the three fuels discussed in the text. Although only one curve for each fluid is shown, each curve was measured four times. The uncertainties relating to the measurements have been discussed in the text.

close. Thus, the distillation curve does not have a large temperature range.

The chromatograms of CTL are more complex (that is, with additional components that are closely eluting), but in fact, some characteristics are similar to those of GTL. There are two dominant peaks throughout the distillation, a methyl nonane and a methyl decane. The peaks are labeled as x-MeC_9 because the resolution of the mass spectrometer does not allow for the precise identification of the place of substitution.

While GTL is composed of largely straight chain alkanes, CTL's composition is dominated by isoparaffinic compounds. This can be seen by the number of peaks in the TICs of CTL versus GTL (see Figure 3). The variations in branching and substitution in the isoparaffinic compounds comprise these many peaks. These branched hydrocarbons also have a higher relative molecular mass than the compounds in GTL and, thus, a lower volatility. This can be seen in the distillation curve of CTL, which is uniformly higher in temperature than that of GTL, indicative of a higher number of lower volatility compounds.

The most striking difference among the chromatograms is seen when one examines the results obtained with the BIO-SPK fuel. In the first drop, the dominant peaks are a methyl octane, a methyl nonane, and *n*-decane. By the 90% distillate fraction, however, all three of those peaks are completely gone. As the volume fraction increases, so does the concentration of heavier straight-chain and branched hydrocarbons. A significant change occurs between the 50% and 70% fractions. The emergent peaks elute at a later time and increase in area. Furthermore, there is a clear presence of much heavier hydrocarbons in the BIO-SPK curve than in either GTL or CTL. While there was a small concentration of *n*-dodecane in the 90% fractions of GTL and CTL, it is the dominant peak in the 70% fraction in BIO-SPK. The peaks elute at an even later time in the 90% fraction. This means that heavier and less volatile compounds are now present at the very end of the distillation curve. In this sample, the early peaks are completely gone, showing only the baseline noise. The *n*-dodecane peak that was dominant in the previous fraction is now a much smaller peak at the beginning of the chromatogram. The dominant peak has become *n*-pentadecane. This composition trend can be directly related to the profile of the distillation curve. The slope of the BIO-SPK curve is much greater than those of the other fuels and covers a wider range of higher temperatures. This result is consistent with the abundance of higher molecular mass compounds, as well as the pronounced differences in the chromatograms between the fractions.

Further work was done to characterize the fuels on the basis of their moiety families. The distillate fractions of the three fuels were examined by a moiety family analysis method that is based on the ASTM Method D-2789. In this method, one uses GC-MS to classify hydrocarbon samples into six different types. The six different moieties are paraffins, monocycloparaffins, dicycloparaffins, alkylbenzenes (or aromatics), indanes and tetralins, and naphthalenes. The results of these analyses (as percent volume fractions) are presented in Table 4a−c. The first line of each of the tables is the analysis of the neat sample (called the composite); this is followed by the results for the distillate fractions. As described in earlier papers, the hydrocarbon type fractions for the composite are generally consistent with the compositions obtained for the rest of the distillate fractions.[33] Taking CTL as an example, the paraffin fraction for the composite sample was found to be 71.6%, while that of the distillate fractions ranged from 69.7% to 73.4%. The uncertainties relating to this analysis are discussed in earlier work.[33]

A graphical representation of these analyses is given in Figure 4. As a function of distillate cut, one can see that, for all three fuels, the percentage of aliphatic compounds, composed of paraffins, monocycloparaffins, and dicycloparaffins, stays relatively constant over the distillation curve. This observation is consistent with our previous examination of the chromatograms of selected fractions (Figure 3), which indicated a high abundance of monosubstituted or linear alkanes. The abundance of cyclic compounds also stays constant throughout the distillation; however, these compounds are at a much lower concentration in all the fuels

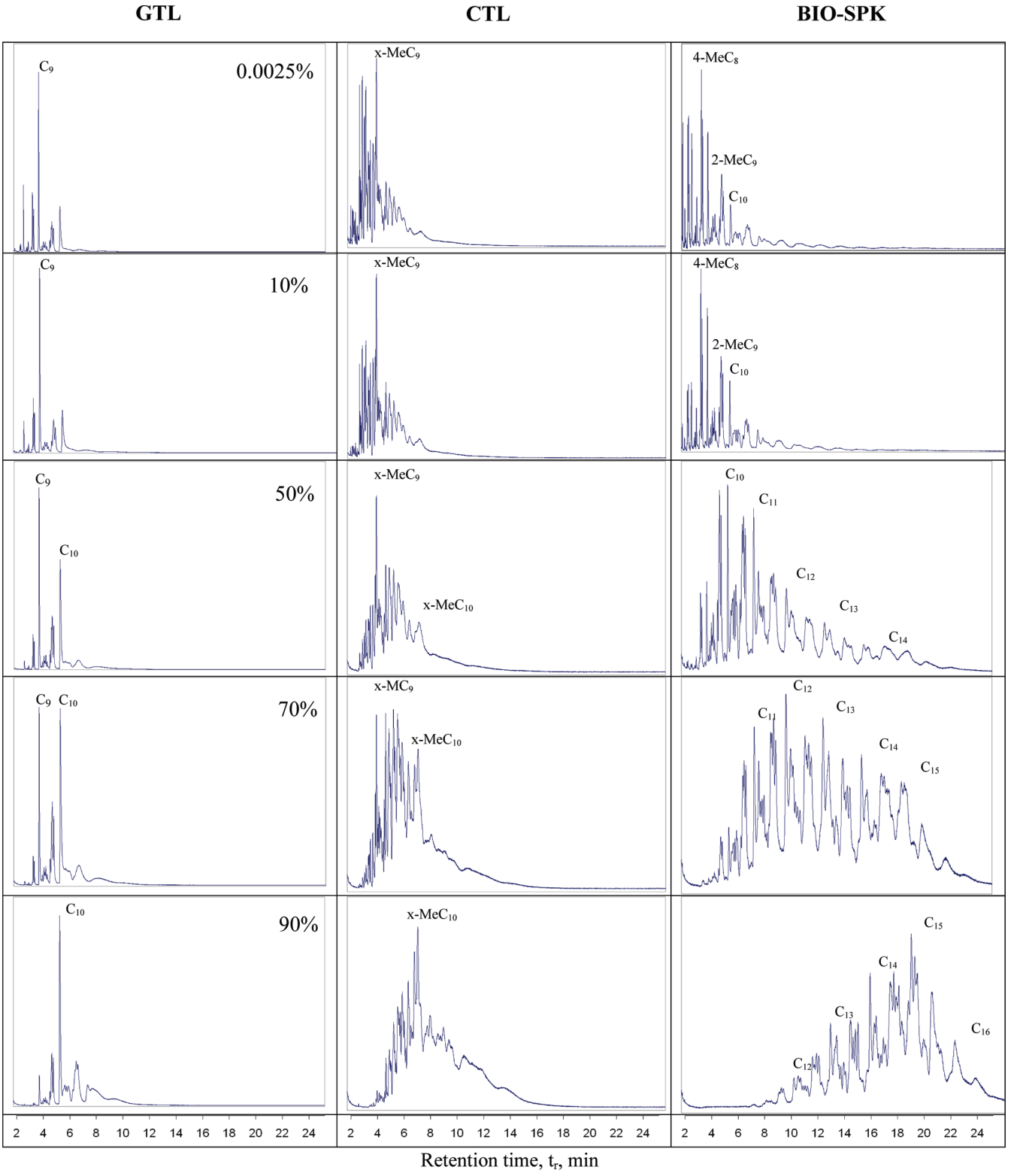

Figure 3. Total ion chromatograms at selected fractions for the three fuels. The chromatography is discussed in the text.

examined here. For example, the percentage of indanes and tetralins is 0.0 to 0.2 for every fraction in every fuel. We also note that there are very few aromatic compounds. This is in contrast to aviation turbine fuels that are derived from petroleum. In those fuels, such as Jet-A and JP-8, the aromatic content is variable but is typically 15% (v/v).[53] One notes upon distillation that the aromatic content decreases from 25% (in the first drop of distillate) to less than 5% at the end of the distillation.

We note that another application of the composition explicit data channel of the ADC is that of a diagnostic on the volatility measurement. If a distillation requires relatively

(53) Detail Specification Turbine Fuel, Aviation, Kerosene Type JP-8 (NATO F-34), NATO F-35, and JP-8 + 100 (NATO F-37); MIL-DTL-83133F, April 11, 2008 and references therein.

Table 4. Summary of the Results of Hydrocarbon Family Calculations as a Function of Distillate Volume Fraction Based on a Modification of ASTM D-2789

(a) GTL

volume fraction (%)	paraffins	monocyclo-paraffins	dicyclo-paraffins	alkylbenzenes	indanes and tetralins	naphthalenes
composite	75.5	21.7	1.0	0.3	0.0	1.5
0.025	75.1	22.7	0.7	0.6	0.0	1.0
10	75.2	22.6	0.7	0.5	0.0	1.0
20	75.6	22.1	0.8	0.5	0.0	1.1
30	75.5	22.2	0.8	0.5	0.0	1.0
35	75.5	22.3	0.8	0.4	0.0	1.0
40	75.6	22.1	0.8	0.4	0.0	1.0
45	75.7	22.0	0.8	0.4	0.0	1.1
50	75.8	21.9	0.9	0.4	0.0	1.0
60	75.6	22.0	0.9	0.5	0.0	1.0
70	75.5	22.0	0.9	0.5	0.0	1.0
80	75.4	22.2	0.9	0.5	0.0	1.0
90	75.5	21.9	1.1	0.5	0.0	1.1

(b) CTL

volume fraction (%)	paraffins	monocyclo-paraffins	dicyclo-paraffins	alkylbenzenes	indanes and tetralins	naphthalenes
composite	72.0	22.4	2.6	1.4	0.1	1.5
0.025	79.7	19.2	0.2	0.2	0.0	0.8
10	76.1	23.4	0.3	0.0	0.0	0.3
20	76.4	23.0	0.3	0.0	0.0	0.3
30	76.5	23.1	0.2	0.0	0.0	0.2
35	76.5	22.6	0.5	0.0	0.0	0.4
40	77.6	22.2	0.1	0.0	0.0	0.1
45	77.7	22.2	0.1	0.0	0.0	0.0
50	76.7	23.1	0.1	0.0	0.0	0.1
60	76.8	22.9	0.2	0.0	0.0	0.2
70	76.7	23.1	0.1	0.0	0.0	0.1
80	75.1	24.3	0.3	0.0	0.0	0.3
90	73.7	25.6	0.1	0.0	0.0	0.6

(c) BIO-SPK

volume fraction (%)	paraffins	monocyclo-paraffins	dicyclo-paraffins	alkylbenzenes	indanes and tetralins	naphthalenes
composite	70.4	22.6	3.1	1.0	0.2	2.6
0.025	80.4	16.2	0.0	0.8	0.1	2.5
10	75.9	20.3	1.9	0.4	0.0	1.6
20	74.3	20.3	2.7	0.8	0.0	1.9
30	73.8	20.3	3.2	0.6	0.0	2.0
35	72.6	21.3	3.3	0.7	0.0	2.1
40	73.0	20.8	3.2	0.7	0.0	2.2
45	73.4	20.6	3.0	0.6	0.0	2.4
50	73.5	20.8	2.9	0.4	0.0	2.3
60	73.9	20.5	2.8	0.3	0.0	2.5
70	74.5	20.4	2.5	0.1	0.0	2.5
80	74.3	19.8	2.6	0.4	0.0	3.0
90	75.1	19.7	2.3	0.2	0.0	2.8

high temperatures to complete, there is always the potential of cracking of components present in the distillate. This can be monitored by noting the onset of emergent cracking products, with reference to thermal decomposition reaction kinetics measurements on the same or similar fluids.[54−60] No such effects were present in the composition measurements in these distillations.

Distillate Fraction Energy Content and Enthalpy Calculations. As we have previously demonstrated, it is possible to supplement the distillation curve with thermochemical data by use of the information available from the composition explicit data channel.[61] This is significant because, in an engine, the fuel undergoes droplet combustion, and a process similar to distillation takes place as the oxidation reactions occur. We calculate a fractional enthalpy of combustion based on the measured mole fractions of the individual components in the distillate cuts. One simply multiplies the

(54) Andersen, P. C.; Bruno, T. J. Thermal decomposition kinetics of RP-1 rocket propellant. *Ind. Eng. Chem. Res.* **2005**, *44* (6), 1670–1676.
(55) Andersen, W. A.; Bruno, T. J. Rapid screening of fluids for chemical stability in organic Rankine cycle applications. *Ind. Eng. Chem. Res.* **2005**, *44*, 5560–5566.
(56) Widegren, J. A.; Bruno, T. J. Thermal decomposition kinetics of the aviation fuel Jet-A. *Ind. Eng. Chem. Res.* **2008**, *47* (13), 4342–4348.
(57) Widegren, J. A.; Bruno, T. J. Thermal decomposition of RP-1 and RP-2, and mixtures of RP-2 with stabilizing additives. *Proc. 4th Liquid Propulsion Subcommittee*, JANNAF, December 2008.
(58) Widegren, J. A.; Bruno, T. J. Thermal decomposition kinetics of propylcyclohexane. *Ind. Eng. Chem. Res.* **2009**, *48* (2), 654–659.
(59) Widegren, J. A., Bruno, T. J., Thermal decomposition kinetics of the kerosene based rocket propellants 2. RP-2 stabilized with three additives. *Energy Fuels* In press.
(60) Widegren, J. A.; Bruno, T. J. Thermal Decomposition Kinetics of Kerosene-Based Rocket Propellants. 1. Comparison of RP-1 and RP-2 *Energy Fuels* In press.

(61) Bruno, T. J.; Smith, B. L. Enthalpy of combustion of fuels as a function of distillate cut: application of an advanced distillation curve method. *Energy Fuels* **2006**, *20*, 2109–2116.

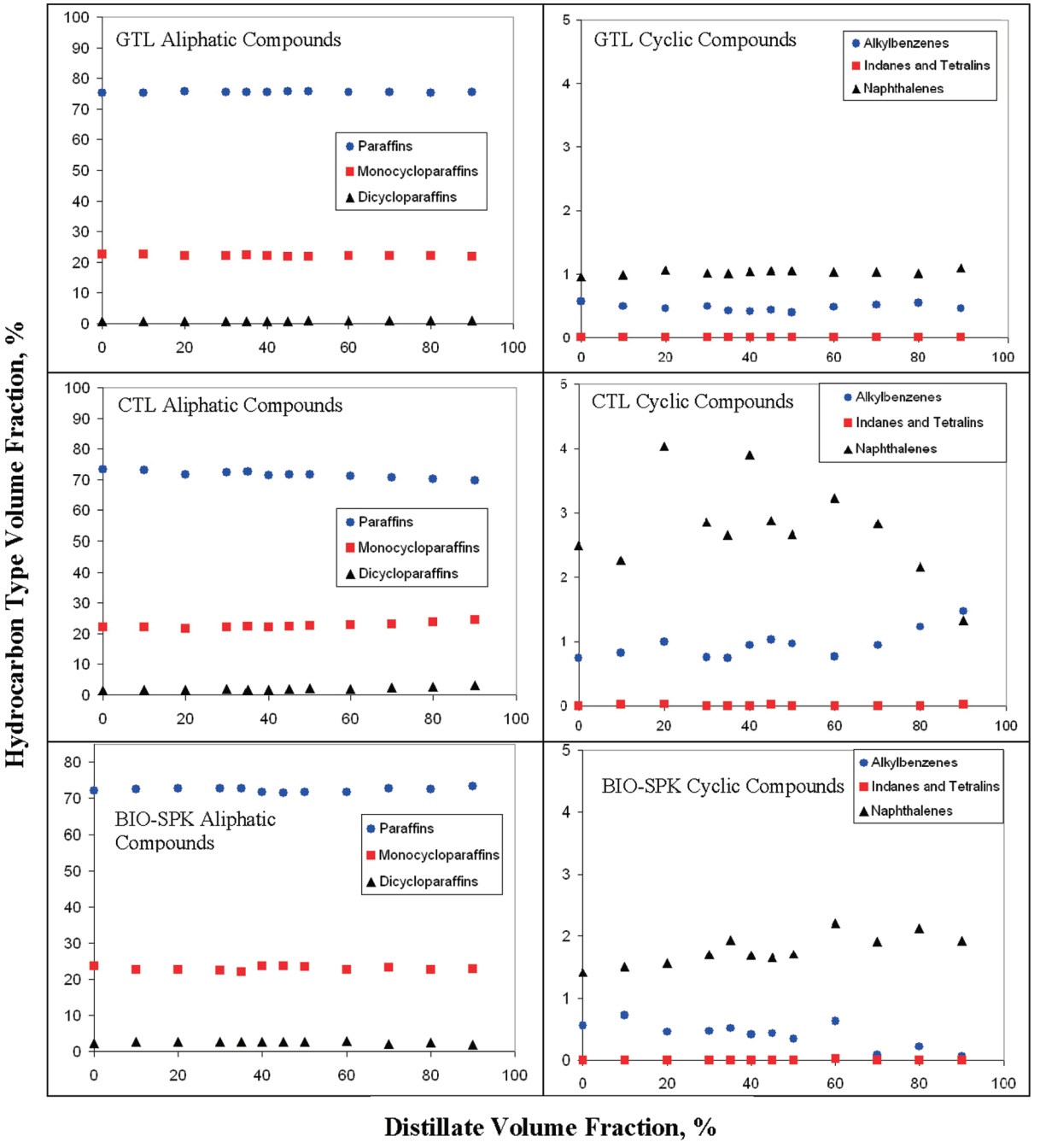

Figure 4. Graphical representation of the aliphatic and cyclic compounds determined by a moiety family analysis using a modification of the mass spectral analysis embodied in ASTM D-2789. Uncertainties are discussed in the text and in the cited references.

measured mole fraction by the pure component enthalpy of combustion. The enthalpy of combustion of the individual (pure) components is taken from a reliable database compilation.[62] We have previously presented a very detailed discussion of the uncertainty of the composite enthalpy of combustion derived from this procedure.[33,61] The major sources of uncertainty that were considered were (1) the neglect of the enthalpy of mixing, (2) the uncertainty in the individual (pure component) enthalpy of combustion as tabulated in the database, (3) the uncertainty in the measured mole fraction, (4) the uncertainty posed by very closely related isomers that cannot be resolved by the analytical protocol, (5) the uncertainty introduced by neglecting components present at very low concentrations (that is, uncertainty associated with the chosen area cutoff), (6) the uncertainty introduced by a complete misidentification of a component, (7) the uncertainty in quantitation introduced by eluting peaks that are poorly resolved, and (8) the uncertainty introduced when experimental data for the pure component enthalpy of combustion are unavailable (and the Cardozo equivalent chain model must be used).[63]

(62) Rowley, R. L.; Wilding, W. V.; Oscarson, J. L.; Zundel, N. A.; Marshall, T. L.; Daubert, T. E.; Danner, R. P. *DIPPR Data Compilation of Pure Compound Properties*; Design Institute for Physical Properties AIChE: New York, 2004.

(63) Cardozo, R. L. Prediction of the enthalpy of combustion of organic compounds. *AIChE J.* **1986**, *32* (5), 844–848.

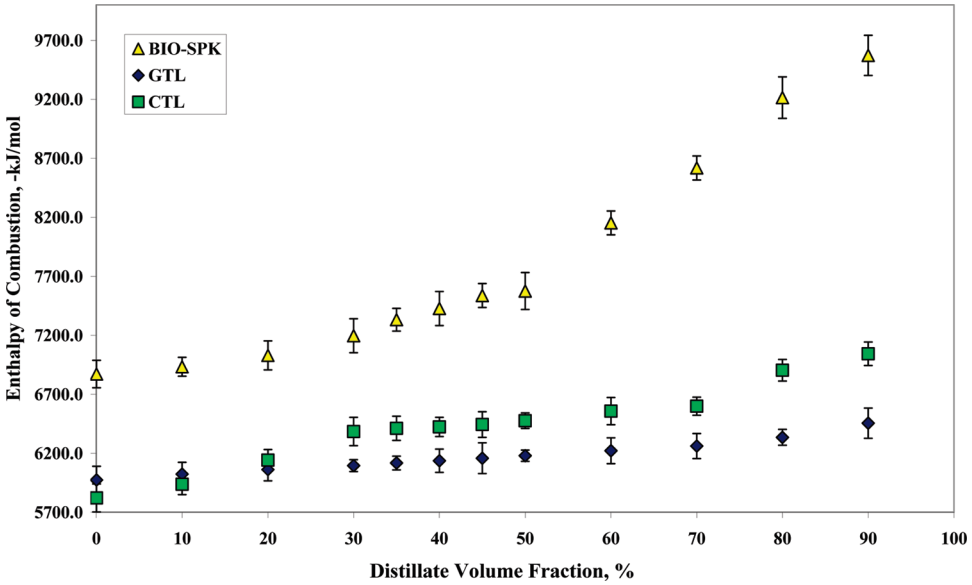

Figure 5. Enthalpy of combustion for the three fuels, presented on a molar basis as a function of distillate cut. The uncertainties are discussed in the text.

Table 5. Composite Enthalpy of Combustion, Presented in −kJ/mol, of Selected Distillate Fractions of Each of the Three Fuels[a]

volume fraction (%)	GTL	CTL	BIO-SPK
0.025	5974 (230)	5821 (240)	6871 (230)
10	6024 (200)	5937 (180)	6933 (160)
20	6062 (190)	6142 (180)	7029 (250)
30	6095 (100)	6384 (240)	7196 (290)
35	6117 (110)	6411 (200)	7332 (200)
40	6136 (200)	6423 (160)	7427 (290)
45	6158 (260)	6443 (220)	7536 (200)
50	6179 (90)	6476 (130)	7575 (310)
60	6221 (220)	6557 (230)	8152 (200)
70	6261 (210)	6599 (150)	8618 (200)
80	6335 (140)	6903 (180)	9215 (250)
90	6455 (260)	7043 (200)	9572 (340)

[a] Uncertainties are provided in parentheses.

As we noted above, it is usually not necessary to include all the components in the calculation. The components that we selected in this work are those that were present in excess of 2% of raw, uncorrected chromatographic peak area counts. The mole fractions of these components were then determined from the areas by standardization. The composite enthalpy of combustion of the distillate fraction was then determined by

$$-\Delta H_c = \sum x_i(-\Delta H_i) \quad (1)$$

where $-\Delta H_c$ is the composite enthalpy of combustion of the distillate fraction, x_i are the mole fractions of the selected components of each distillate fraction, and $-\Delta H_i$ are the pure component enthalpies of combustion.

For the three fluids studied, we present the enthalpy in negative kilojoules per mole as a function of the distillate volume fraction in Table 5 and Figure 5. For GTL and CTL, the enthalpies change modestly as the distillation proceeds. These enthalpy of combustion data mirror the distillation curves, which are also relatively flat. This is also consistent with the chemical analyses discussed earlier. Moreover, the enthalpies of combustion of GTL and CTL are relatively close; indeed, early in the distillation curves, they are within experimental uncertainty. As the distillation proceeds beyond the 50% distillate fraction, the CTL shows a higher enthalpy compared to the GTL. This divergence is also consistent with the chemical analysis of these later fractions.

Table 6. Composite Enthalpy of Combustion, Presented in −kJ/g, of Four Distillate Fractions of Each of the Three Fuels[a]

volume fraction %	GTL	CTL	BIO-SPK
0.0025	44.4 (1.7)	44.3 (1.7)	44.2 (1.5)
10	44.4 (1.4)	44.3 (1.3)	44.2 (1.0)
50	44.4 (0.7)	44.2 (0.9)	44.1 (1.9)
90	44.4 (1.7)	44.2 (1.2)	44.0 (1.5)

[a] Uncertainties are provided in parentheses.

A marked difference can be seen in the enthalpy of combustion for the BIO-SPK as compared with those of the GTL and CTL. Through the 20% distillate fraction, the enthalpy of combustion exhibits a gentle increase (similar to the behavior observed for GTL and CTL). In this region, the enthalpy is higher than that of the GTL and CTL by approximately 500 kJ/mol. After the 30% distillate fraction, the enthalpy begins to slowly climb. Beginning at the 50% distillate fraction, there is a rapid and steep climb until the final 90% fraction. We note that this is consistent with the composition measurement. After the 50% fraction, the measured peaks shifted dramatically to much longer retention times, and the quantity of heavier hydrocarbons (as measured by the area counts) significantly increased. This trend can be seen continuing into the 90% distillate fraction chromatogram. We observe a large difference in enthalpy at the end of the distillation among the three fluids. At the 90% fraction, the enthalpies of GTL, CTL, and BIO-SPK are −6455 kJ/mol, −7043 kJ/mol, and −9572 kJ/mol, respectively.

Although we express the enthalpy of combustion on a molar basis to facilitate calculations, other units are sometimes preferred. In practical terms, a mass or volume basis is often desired by aircraft operators. The conversion to a mass basis is simple, requiring only the relative molecular mass of each component used in the calculation. We present the enthalpy of combustion on a mass basis (in −kJ/g) of selected distillate cuts for the three fuels in Table 6. Presenting the

Table 7. Composite Enthalpy of Combustion, Presented in −kJ/mL, of Four Distillate Fractions of Each of the Three Fuels[a]

volume fraction %	GTL	CTL	BIO-SPK
0.0025	31.9 (1.3)	31.9 (1.3)	32.6 (1.1)
10	32.0 (1.1)	32.0 (0.9)	32.6 (0.8)
50	32.2 (0.5)	32.4 (0.6)	32.9 (1.4)
90	32.4 (1.3)	32.6 (0.9)	33.8 (1.1)

[a] Uncertainties are provided in parentheses.

enthalpies of combustion on a volume basis is more uncertain, because the density of each compound is necessary. While the density of the fuel itself varies little with composition, the density of the individual components varies significantly with temperature. Moreover, there is often a lack of reliable density data at the temperatures of interest, especially reference quality data. These additional contributions to uncertainty must be considered upon conversion to the volume basis. For each of the fluids measured in this work, we present in Table 7 the enthalpy of combustion on a volume basis (in −kJ/mL) of the same selected distillate fractions as in Table 6. The temperature basis for this table was chosen as 25 °C. We note that, on these more practical bases, the energy content is far more uniform over the distillation curve. This is primarily due to differences in density of the three fuels, and changes in density during the course of distillation.

Conclusion

In this paper, we have presented our examination of the composition of three alternative synthetic isoparaffinic kerosene turbine fuels (one of which is renewable) with the advanced or composition-explicit distillation curve method. The advanced distillation curve method provided for accurate measurements that are suitable for equation of state development. Furthermore, we were able to obtain detailed compositional data as a function of distillate cut for each of the fuels. We analyzed the distillate fractions of each fuel for specific component information with the GC-MS. Finally, we combined the component information with thermochemical data for an explicit measure of the energy content of each fraction. The fluids made from natural gas and coal had a similar volatility behavior, while the bioderived fluid made from brown grease was far less volatile. The energy content on a molar basis mirrored the volatility behavior.

Acknowledgment. A Professional Research Experience Program undergraduate fellowship is gratefully acknowledged by E.B., and a National Academy of Sciences/National Research Council postdoctoral fellowship is gratefully acknowledged by T.M.L. We acknowledge the Propulsion Directorate of the Air Force Research Laboratory, Wright Patterson Air Force Base, for the samples of fuel measured in this effort.